Assisted Radiological Stabilization and Monitoring of Radon Fluxes and Gamma Irradiations of Residues from the Processing of Uranium Ore of Arlit Mines (Northern Niger) Using Multivariate Statistical Methods and the Geotechnical Approach

I. Elhadji Daou[1]*, S. Harouna[2], A. Maman Hassan[2]**, C. Przemysław[3], S. Marcin[3], A. Tankari Dan Badjo[4]

[1]*Department of Mining Engineering and Environment, School of Mines, Industry and Geology of Niamey, BP 732 Niamey, Niger*
[2]*Department of Geosciences, School of Mines, Industry and Geology of Niamey, BP 732 Niamey, Niger*
[3]*Department of Soil Science and Landscape Management, Faculty of Earth Sciences and Spacial Management, Nicolaus Copernicus University, ul. Gagarina 11, 87 - 100 Torun, Poland*
[4]*Department of Soil Science, Faculty of Agronomy, Abdou Moumouni University, BP 10960 Niamey, Niger*
Corresponding author: updaou@yahoo.fr
**Corresponding author: abdourazakoum@gmail.com*

Abstract
This study concerns the radiological stabilization of radon fluxes and gamma irradiations of the tailings resulting from the treatment of uranium ore from Arlit mines. The results of this study showed that the permeability values at temperature T of the Tejia Clay and Abinky Sandstone used for the reclamation and containment of the tailing pits resulting from the ore processing in the study area vary between $0.005.10^{-7}$ to $0.0016.10^{-7}$ m/s. At a temperature of 20℃ these values are lower than those measured previously and vary between $0.003.10^{-7}$ and $0.0016.10^{-7}$ m/s. The porosity values of samples vary between 14.29 and 17.92 with an average of 16.13. These low permeability and porosity values indicate that the Tejia Clay and Abinky Sandstone are sufficiently suitable for the containment of tailings from uranium ore processing in the study area. The measurements made of gamma radiation and radon are very low after the 2m cover. The average attenuation is between 70% and 92%. Radon is down by 70% for a 94% decrease in gamma radiation in μSv/h. The principal component analysis allowed to identify two main groups of factors. The first group of factor which accounts for 46.84% of the total variance is mainly related to a strong positive loading of gamma radiation and a strong negative loading of the altitude values. Factor 2 which accounts for 38.191% of the total variance is mainly related to a strong positive loading of humidity, temperature and a medium positive loading.

1. Introduction

The energy needs of today's world are becoming problematic. Indeed, one of the sources of electricity, nuclear energy, is entirely dependent on uranium [1]. It is this dependence that leads most of the major industrialists to look for uranium deposits wherever they can be found, especially in developing countries where workers' rights are hardly respected. The uranium mining operations of the early 20th century have left behind memories of negative impacts on health, safety and the environment that are difficult to dislodge [2]. Uranium is a heavy metal that has the potential to cause a variety of adverse health effects, ranging from kidney failure to decreased bone growth to DNA damage [3,4].

The components (atoms) of uranium are unstable, so it must undergo various transformations to be made more radioactive for use in reactors as nuclear fuel. The decay of this fuel produces heat that boils water, producing steam that turns turbines, which produce electricity. Because uranium is both toxic and radioactive, it is difficult to assess the relative contributions of each of these characteristics to its toxicological profile. Effects of low-level radioactivity include cancer, decreased life expectancy, and subtle changes in fertility or offspring viability, as evidenced by animal studies and data on Hiroshima and Chernobyl survivors [1,5,6]. Uranium is subject to a wide range of interpretations and concerns related in large part to its rather chequered history. Over the years, people's perception of the word uranium has been associated with nuclear power and has thus been influenced by its military use and also by the many nuclear accidents around the world. The uranium decay process generates new elements (Radium 226, Radon 222, Polonium 210 and Thorium 230) with varying degrees of radioactivity depending on their concentration [7]. In uranium mines, uranium ore tailings from the processing of ore extracted from underground or open-pit mines constitute, in addition to physical, visual and radiological pollution, a major public health problem. Indeed, the exponential increase in mine tailings contributes to the proliferation of radiological risks and the contamination of air, soil and groundwater. Uranium mining produces waste that exposes both humans and the environment to threats that are imperceptible to the naked eye and in most cases manifest themselves over the long term. They can have a strong influence on the economic profitability expected by the state and the mining companies. Radioactivity occurs when the nucleus of an unstable atom such as uranium loses energy in the form of a type of ionizing radiation, either alpha, beta or gamma [8,9].

In Niger, uranium mines extract hundreds of thousands of tons of uranium ore each year to produce a few thousand tons of uranium concentrate. The ore extracted from these mines goes to a plant for processing. This processing consists of mechanical operations, including drying, crushing and screening, and chemical attack. After processing, the tailings are sent to a storage area and the main risks associated with this storage are radiological, environmental and safety risks. In addition to the direct environmental impacts associated with the exploitation and processing of ores, residual tailings are also responsible for environmental pollution, in particular water and soil contamination, but also acid mine drainage when they are in contact with water and/or air [10]. The best method so far used to treat uranium ore tailings is mechanical covering with any rock. In the case of the Nigerien mines, which are companies under Nigerien law and whose corporate purpose is the exploitation of uranium deposits, several test beds were carried out to find the most optimal covering method. This optimal treatment method would provide effective containment of radioactivity at an optimal cost. The tests were conducted on slopes with in situ materials. The materials used in these tests are Tejia clay and Abinky sandstone. Tejia clay is a clay that has all the qualities required to be used in this type of capping. Abinky sandstone is used for mechanical protection against rain. At the level of the Akouta Mining Company (COMINAK), for a global treatment of the slopes, it will be necessary to carry out important reprofiling works to give a regular shape to the surface of the tailings; while at the Société des Mines de l'Air (SOMAIR), it is this radon which constitutes a real source of contamination of the environment and can reach very high concentrations with consequences on health. Radon-222 is a radioactive gas that is a daughter product of the radioactive decay sequence of uranium-238 and its daughter product, radium-226 [11]. Exposure to ionizing radiation from radioactive materials can be harmful to human health [12,13,14]. Current international radiation protection standards set dose limits at 20 mSv yr^{-1} for radiation workers and 1 mSv yr^{-1} for members of the public for radiation doses from duly authorized practices involving the application of radiation and/or the handling of radioactive substances [15]. materials Apart from uranium mines, it is also found at high levels in some areas,

especially if houses are built on granite subsoils. Radon is classified as a definite human lung carcinogen by the World Health Organization's International Agency for Research on Cancer [16]. Its inhalation can therefore lead to the development of lung cancer as shown by numerous data from animal experiments as well as epidemiological studies conducted initially in uranium miners [17].

The present study thus concerns the radiological stabilization assisted by radon fluxes and gamma irradiations of the tailings resulting from the processing of uranium ore from the Arlit mines. This city located in the north of Niger is one of the main uranium mining cities in the world. The population of this city in general and the employees of the mine in particular are confronted with a serious health problem linked on the one hand to the effects of radiation and on the other hand to the pollution due to fine mineral particles likely to cause numerous respiratory and cardiovascular diseases [18].

2. Materials and methods

2.1 Presentation of the study area and the geological context

The urban commune of Arlit is located in the Agadez region, between latitudes 18° 24' 22" N and 21° 11' 03" N and meridians 5° 47' 54" E and 8° 02' 28" E. It occupies the northern, desert part of the Republic of Niger with an arid, hot and dry climate. It is limited to the east by the rural commune of Iférouane, to the west by the rural commune of in Gall, to the south by the rural commune of Dannat, to the south-east by the rural commune of Gougaram and to the north by Algeria and has fifteen districts: Cité SomaÏr, Zongo, Wadata, Sahel, Tamesna, Boukoki Tanesna, Boukoki Sud, Boukoki Est, Carré SNTN, Carré Nouveau Marché, Compagnie Madawela, Cité Akokan, Akokan Carré, Quartier Administratif and Takriss [19]. This formerly uninhabited city, has a population estimated in 2007 at 99,000 inhabitants including 28,000 inhabitants in the mining cities and 71,000 in the induced cities [20]. The municipality has in 2018 more than 200,000 inhabitants following the population growth. The city of Arlit is located in the Saharan zone which covers 77% of the country where the average annual rainfall is less than 150 mm. The region is desert, dry and hot, characterized by an average annual temperature that varies between about 15°C and 35°C, with an average of 28°C. Maximum temperatures can exceed 40°C from March to October and approach 45°C from May to July. Nights are generally cool during the cold season with temperatures below 20°C. The warmest temperatures of the year are observed in the months of May and June with an average of 34.2°C at this time. The coolest temperatures are observed in the month of January with the average temperature is 18.8 °C [21,22].

The study area is located in the Tim Mersoi sedimentary basin. This basin is a sub-basin of the Iullemenden Basin (Phanerozoic) developed on the basement of the West African Proterozoic shield. The Iullemenden Basin covers most of the western part of the Niger Republic and extends into Algeria (Tin Serine Basin), Mali, Benin and Nigeria. It opens and deepens towards the south and west. The Tim Mersoi Basin forms an appendage at the N-E end, and is located in a N-S trending "gutter" of the basement [23]. The stratigraphic division of the Arlit region includes the Precambrian composed of crystalline and crystallophyllous rocks; the Permo-Carboniferous including the Upper Tagora, Lower Tagora and Teradah series. Each of these three Permo-Carboniferous series begins with fluvio-glacial sandstones at Terag in the Teradah, a fluvio-estuarine formation at Guézouman in the Lower Tagora (with the radioactive conglomerate of Teleflak at the base) and fluvio-deltaic at Tarât, in the Upper Tagora the Permian, which corresponds to two cycles, including successively a fluvial episode (sandstones of the Izégouande and Tamamaït series) and a lacustrine episode (mudstone of the Téjia and Moradi series); the Triassic represented by the fine sandstones of the Téloua 1 and the Lower Cretaceous constituted by the lacustrine clay formation of the Irhazer [24,25].

The mining district of the town of Arlit records the deposits exploited by the Akouta Mining Company (COMINAK) and by the Société des Mines de l'Aïr (SOMAÏR). These uranium deposits are located on the eastern edge of the Tim Mersoi intracratonic basin near the Aïr massif. These mines are located in the area between latitudes 18°35'N and 18°43'N and longitudes 7°15'E and 7°20'E for COMINAK and more precisely between 7°15' and 7°30' East longitudes, 18°30' and 19° North latitudes for SOMAIR. (**Figure 1**) Each of these deposits begins with a sandstone formation, fluvio-glacial in the Teragh in the Terada, Fulvio-deltaic in the Guezouman in the Lower Tagora, with the radioactive conglomerate of Teleflak at its base, and in the Tarat in the Upper Tagora [26].
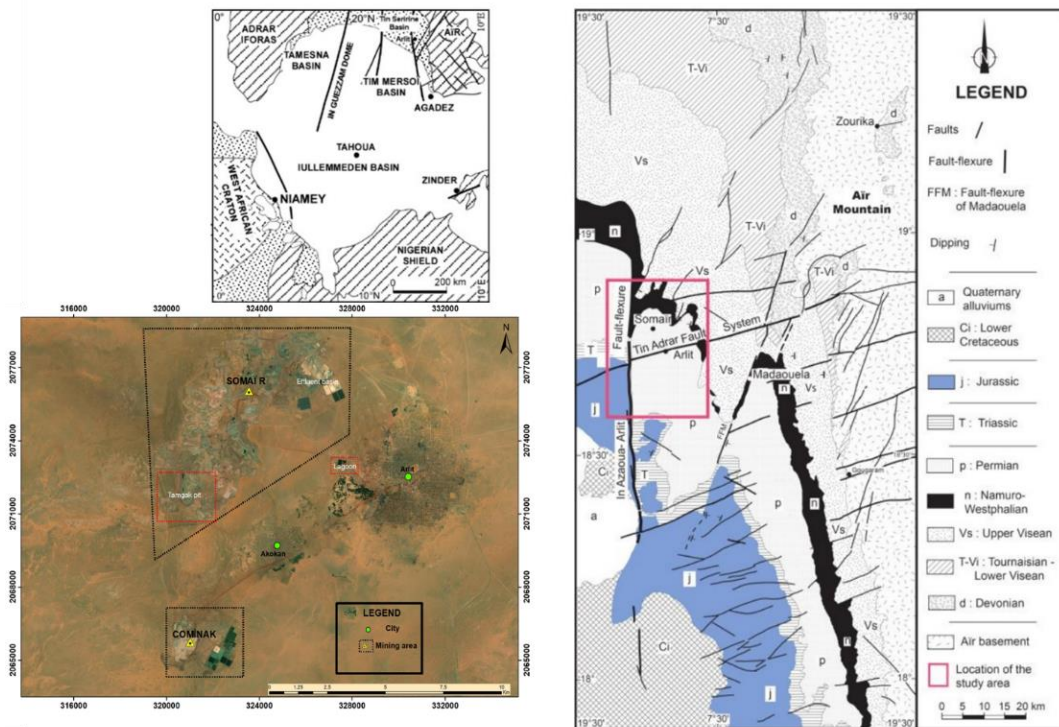

Figure 1. Presentation of the study area and geological context [27]

2.2 Determination of the Permeability of Tejia Clay and Abinky Sandstone

In the majority of the flows in porous medium, it is the law of [28] which is applied. Indeed, the conditions of application of this law are generally verified, because the speed of flow when it takes place hardly exceeds the 1cm/s. The flow of water in the ground is carried out by the pores with variable ways, it is for this reason that the real speed of the flow makes intervene the porosity of the ground. This real speed allows to determine the average time t necessary for a water particle to cross a soil cylinder of length L. It is given by the following formula [29]:

$$V = K \times i \qquad\qquad\qquad\qquad \textbf{Eqn. 1}$$

Where i is the head loss per unit length of the porous medium or hydraulic gradient.

In the present study, permeability values were determined by the laboratory method. This method uses the Darcy model, by means of a direct compact permeameter. This apparatus consists of a cylinder closed by a bottom and a top in which the material under study is compacted by hand. The bottom is then replaced by a watertight base, fitted with a porous stone. Two rubber gaskets ensure the tightness of the pot. A grooved connection at the base of the apparatus allows the connection to water, the outlet through the sample being observed by means of a tube mounted on the lid.

From the set-up, measurements with the permeameter, the quantities such as the section of the sample S which corresponds to the section of the mould used, the height L of the sample; the hydraulic load created H, the volume of water Q collected after a certain time of waiting for the eventual flow to take place and the time necessary T to collect the volume Q are known. The permeability is therefore calculated using the following relationship:

$$K = \frac{Q \times L}{S \times T \times H}$$ **Eqn. 2**

Where H is the hydraulic load created, L is the height L of the sample, T is the time required T, S is the cross section of the mould used and Q is the volume of water.

However, since the conditions of the experiment involve the temperature of the liquid, the viscosity and pressure drop are a function of this temperature, as is the permeability coefficient obtained. To compare the results, the value of this coefficient is brought back to the temperature of $20^o C$ by the formula :

$$K_{20} = K \times \frac{\eta_T}{\eta_{20}}$$ **Eqn. 3**

Where η is the dynamic viscosity of water at $T°C$ and at 20°C.

2.3 Determination of porosity values

The permeability coefficient is a measure of the soil porosity under the given hydraulic gradient conditions. To determine the total porosity, it is sufficient to measure the void index of each sample (Stengel 1979). A pycnometer is used to determine the specific gravity of the soil grains.
Porosity is expressed by the following formula [30]:

$$e = \frac{\gamma_s}{\gamma_d} - 1$$ **Eqn. 4**

$$n = \frac{e}{1+e}$$ **Eqn. 5**

Where: e void index of the soil studied and n is the soil porosity.
Thus, n can be deduced from the following formula:

$$n = \frac{\gamma_s - \gamma_d}{\gamma_s}$$ **Eqn. 6**

with γ_d et γ_s representing respectively the dry density at the Proctor optimum and the specific gravity of the soil grains.

2.4 Gamma irradiation measurements

Gamma radiation measurements (expressed in c/s and µSv/h) are made with a colimated GAMMA SPP with a 20x20m mesh before and after the installation of the cover materials. The colimated GAMMA SPP is a device used for the detection of total gamma radiation. In general, it is used in Uranium prospecting (counter plan, ground control and positioning of airborne K, U, Th anomalies or total counting); in mining prospecting (mapping of clay or hydrothermal alteration zones, assistance and/or complement to geological mapping); in monitoring and follow-up of storage sites and in radiometric follow-up after rehabilitation of industrial or mining sites. For all measurements, gamma photons produced by a radioactive source react with the material of a scintillator creating photons detected by a photomultiplier [31,32]. The number of photons detected is proportional to the number of decays initially emitted.

2.5   *Radon flux measurements*

Tailings from the processing of uranium ores contain radium-226 in relatively large quantities. This radionuclide generates, by radioactive decay, a gas that is itself radioactive, radon-222 (Ferry 2000). At COMINAK, radon flux measurements (expressed in Bq/m3 and in at/m2/s) are taken on the tailings pits at a 20x20m grid before and after the cover materials are put in place.

At SOMAIR, radon concentration measurements are made by sampling a volume of air representative of the atmosphere under study and detecting the radiation whose emission accompanies the successive radioactive decays of radon isotopes and their descendants. The activity of a given quantity of a radionuclide is proportional to the number of atoms that make up that quantity. The proportionality coefficient is called the radioactive constant, symbol λ expressed in s-1. The activity A is measured in becquerels [33,34]. We have the equality:

$$A = \lambda N \ (Bq) \hspace{4cm} \textbf{Eqn. 7}$$

N : number of atoms ; λ : radioactive constant in s-1 .

This is how the activity of radon gas is calculated, and the result is expressed in becquerels per cubic meter (Bq/m3) of air. However, radon gas is never present without its progeny.

During this study, two types of measurements were carried out: one-time measurements carried out over a period of time, which provide a "snapshot" of the situation at a given moment, and continuous sampling, which makes it possible to monitor changes in concentration over time.

For point measurement, the Volumetric Potential Alpha Energy Meter (VAPEM) is used. It is a device for measuring the potential alpha activity of short-lived radon-222 progeny in air and consists of the following components: a metal case containing the battery, pump, detection module, sensors and an electronic board; a sampling filter placed in a disposable cardboard box; and a holder to secure the sampling filter during the sampling phase. The MEAP V also uses a rotary vane pump to draw in air. The sampling flow rate (about 6 litres per minute) is calculated from the measurement of the vacuum and the rotation speed of the pump. Temperature and atmospheric pressure compensation is integrated. In this way, the volume taken is accurately calculated before being used in the calculation of the Alpha Potential Volumetric Energy (APVE). But for the measurement to be valid, a minimum volume must be withdrawn.

For continuous measurements, the principle consists in continuously sampling a known and representative volume of air in-situ by free convection in order to permanently detect the radiation emitted by radon and its descendants. The device used to perform these measurements is the ÆR radon monitor. The ÆR radon monitor is a device for measuring the volumetric activity of radon and its short-lived progeny in the air and is composed of the following elements: an aluminium case integrating the battery, the pump, the detection module, the sensors, as well as an electronic card; a small orifice through which the ambient air penetrates by diffusion inside the device and a super contrast e-paper screen. This screen permanently displays: the temperature, in degrees Celsius; the humidity, in %; the radon activity volume, in Bq/m3; the time range corresponding to the radon measurement displayed and an emoticon whose mood indicates whether the radon level measured at the last measurement point is below or above the regulatory threshold. The values are updated at each measurement period. During the sampling, the ambient air penetrates by diffusion inside the device through. A photodiode detects the particles emitted by decay and transforms them into electrical impulses. These electrical impulses are counted by an electronic card during a time range called "measurement period". At the end of each measurement period, the electronic board calculates the radon concentration according to the number

of electrical pulses, the measurement period and the calibration coefficients of the device. In addition to the above mentioned parameters, two (2) other metrological parameters are taken into account in the present study: temperature and humidity.

Multivariate statistical methods such as correlation analysis and principal component analysis were used using SPSS software to determine the relationship between radon concentrations, gamma radiation values, elevation values, temperature values and humidity values.

3. Results and Discussion

3.1 Variation of Radon Concentrations, Gamma Radiation and Climatic Parameters in the Work Environment

The amounts of radon or its progeny cannot be measured directly. As a rule, they are below the sensitivity of the best instruments used. However, the number of decays of each radionuclide per unit of time or the concentration of air in potential alpha energy (PAE) expressed in joules per cubic metre (J.m-3) or potential alpha energy by volume (PAEv) can be measured. In fact, with each decay, an alpha or beta particle is emitted, sometimes accompanied by the emission of a gamma photon. Each of these emissions can be detected by different types of counters. The measurement is therefore based on the sampling of a volume of air representative of the atmosphere studied and the detection of the radiation whose emission accompanies the successive radioactive decays of the radon isotopes and their descendants. Both continuous and point measurements were implemented for this study. For the continuous radon measurements, the AER is equipped with probes allowing it to measure temperature and humidity as well as wind speed and direction. All meteorological data is provided by the company's control tower. Indeed, the company has a weather station where all parameters are continuously recorded. The following **Table 1** presents the results of descriptive statistical analysis of the meteorological data, the altitudes of the measurement points and the measurements made of the evolution of the volumetric activities of radon and gamma radiation within the SOMAIR pit recorded from June 2021 to May 2022. The analysis of this Table 1 shows that the radon concentration values vary between 0 and 7400 Bq/m3 with an average of 804.88 Bq/m^3. It can be seen that most of the measured radon concentration values are well above the permissible standard. Radon exposure remains a major environmental determinant of health, as it is notably the second leading cause of lung cancer after smoking [35,36,37,38]. The analysis of radon-related health risk is complex because cumulative exposure is the result of a variable concentration of air in a given location weighted by the length of stay in that location. Indeed, studies have shown that even domestic exposure to this gas would result in between 1000 and 3000 lung cancer deaths in France per year [39], which represents about 10% of lung cancer deaths [40,41]. As for the γ-gamma radiation values, they vary from 1.26 to 4.16 mS/h with an average of 1.867 mS/h. The values of humidity and temperature measured during this period vary respectively from 6 to 39% with an average of 17.38 for humidity; and from 26.6 to 49.5 °C with an average of 36.23 °C for temperature.

Table 1. Descriptive statistics of Parameters

Parameters	N	Minimum	Maximum	Mean	Std. Deviation	Variance
Radon (Bq/m3)	266	0	7400	804,88	1218,899	1485714
Temperature(°C)	266	26,5	49,5	36,239	5,6332	31,732
Moisture (%)	266	6	39	17,38	6,624	43,873
γ (mS/h)	266	1,26	4,16	1,8674	1,1131	1,239
Altitude (m)	266	314,3	324	320,932	4,1594	17,301

3.2 Characterization of the Tailings Test Bed and its Containment Procedure

The characteristics of the test bed are as follows: the surface area is 1 ha with a slope of about 7% and the height of the test area is about 15 m, which is a height that gives a good representativeness in relation to the emission of radioactivity. Beforehand, the area defined for the test was earthworked to give it a slope of 5%. The aim of this 5% slope is to determine the behaviour of the board with rainwater, as the slope will be re-profiled during the overall reorganisation. After the earthwork, a radiological counter plan on fixed points (implanted by the topographic section) was carried out to measure the radioactivity of the mother board or original board. These initial radioactivity measurements will be compared to the measurement results after the final cover to determine the containment performance. The edges of the board are staked to avoid any risk of marking by runoff from the surrounding area. The capping is done in four passes, three (3) passes of 0.5m each of Tejia layer and one pass of 0.5m of Abinky layer. In each pass the clay is moistened and compacted to ensure good containment (**Figure 2**).

The reclamation of the slope is carried out by placing the slope on a watertight clay layer with a permeability of $k < 10^{-8}$ m/s ; by placing a geomembrane (liner) on the clay layer to ensure the watertightness of the barrier, then by determining the integrating slope of the slope of the slope not exceeding 30 degrees and allowing to have a safety coefficient $f \geq 1.5$ to have a good stability of the slope and finally by dividing the main slope into several sub-slopes called redans with a slope < 15 degrees. In fact, the width of the sub-slope bench must be around 10 m to allow earthmoving machines to maneuver well. The slope must be covered by two (2) layers, of which the $1^{ère}$ is a waterproof clay layer of about 2m thickness; while the $2^{ème}$ is a sandstone layer of about 50 cm, which aims to break the force of water, and slow down the wind erosion; also these 2 dimensions allow the slope to have a radiological pass in accordance with the regulatory limit. In order to allow the evacuation of rainwater, drainage banks based on riprap and water evacuation chimneys are built on the slope. To collect run-off water, basins sized on the basis of a 100-year flood were dug and devices to control the stability of the slope (inclinometers) were installed. In addition, piezometers were installed all around the redeveloped slope to check watertightness and dosimeters were installed for radiological monitoring.
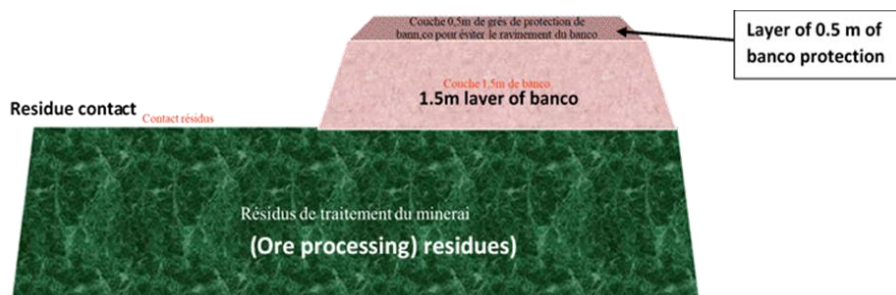

Figure 2. Illustration of a test bed covering a pile of uranium processing tailings

3.3 Permeability and porosity of the Tejia Clay and Abinky Sandstone

Tejia clay and abinky sandstone are the materials used for the reclamation and containment of tailings from the processing of uranium ore in Nigerien mines. They have all the qualities required to be used in this type of covering and for mechanical protection against rain. The immediate analysis consisted in determining certain properties of the materials used, in particular the permeability and porosity for the clay. The following **Table 2** and Table 3 present respectively the values of permeability and porosity calculated within the framework of the present study. The analysis of **Table 2** shows that the permeability values at temperature T vary from $0.005.10^{-7}$ to $0.0016.10^{-7}$ m/s with an average of

$1.33.10^{-8}$ m/s. The permeability values at 20℃ permeability values are lower than those measured previously and vary between $0.003.10^{-7}$ and $0.0016.10^{-7}$ m/s with an average of $1.016.10^{-8}$ m/s. These low permeability values indicate that the samples are sufficiently suitable for the containment of tailings from uranium ore processing in the study area. In addition, it should be noted that the samples did not sink after 72 hours of waiting and were found to be relatively impermeable. Analysis of the **Table 3** shows that the porosity values of the samples analyzed range from 14.29 to 17.92 with an average of 16.13. These low porosity values indicate that these materials are relatively low porosity, i.e. of high compactness. This confirms the impermeability of the tested samples.

Table 2. Pearmeability values of samples

Career	Sample	Permeability KT(m/s)	K20(m/s)
	E1	Waterproof 72 hours after saturation	
Tamou	E2	0,000000005	0,000000003
	E3	0,000000013	0,000000013
	E4	0,000000016	0,000000016
Mean		1,13333E-08	1,06667E-08

Table 3. Porosity values of samples

Samples numbers	Specific gravity	Dry density	Porosity
E1	2,35	1,97	16,17
E2	2,4	1,97	17,92
E3	2,31	1,98	14,29
E4	2,35	1,97	16,17
Mean	2,3525	1,9725	16,1375

3.4 Dose deduction after containment of the tailings area

In 2020 - 2021, the average added dose for the sedentary population (which is the most exposed) is 0.79mSv. This result is obtained with the current situation, i.e. without coverage. In this dose of 0.79mSv, it should be noted that radon accounts for more than 90% of the total all-hazards dose (radon, gamma, dust and dose from food ingestion). Thus, the dose is 0.71mSv in the average of 0.79mSv. **Figure 3** shows the dose deduction added to the environment after the 2m coverage.
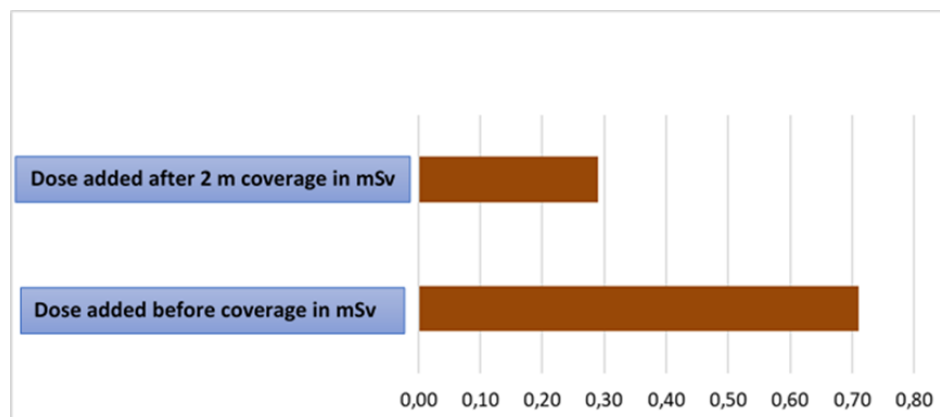

Figure 3. Deduction of doses added to the environment after the 2m coverage

By the deduction method, It was obtained the following results:

- The radon dose added to the environment would be:

$$0,71 mSv - (0,71 mSv * 70/100) = 0,21 mSv$$

- The added dose in gamma + dust + food chain

$$0,79 mSv - 0,71 mSv = 0,08 \; mSv$$

- The total dose added to the environment would be: 0.29 mSv

Table 4 presents the results of the analysis of measurements made on uranium ore tailings from the processing of ore extracted from the Arlit underground and open pit mines. It presents gamma radiation measurements expressed in c/s and µSv/h and radon flux measurements expressed in Bq/m3 and at/m2/s. The gamma radiation and radon measurements are very low after the 2m coverage. On average, the attenuation varies from 70% to 92%. Radon is down by 70% for a 94% decrease for gamma in µSv/h. This proves that the cover is very effective and attenuates considerably the emitted radioactivity, which will not be without consequence in the decrease of the dose added to the environment.

Table 4. Results of measurement analysis on uranium ore tailings from the processing of ore extracted from the Arlit underground and open pit mines

	Rn 222 Volumetric Activity (Bq.m3)	At/m2/s	Colimated in lead (C/S)	Colimated in lead µs/h
Measuring board meter	1430557,98	7550167,1	695,46	1,48
Cover measurement 2 m	434864,5	2295118,2	96	0,08
Mitigation	-70%	-70%	-86%	-94%

The following **Figure 4** is a representation of the radon activity volume and gamma radiation dispersion as a function of the thickness of the cover made in four passes, namely the 3 passes of 0.5m each of Tejia layer and one pass of 0.5m of Abinky layer. In each pass, the clay is moistened and compacted to ensure good containment. The analysis of this figure shows a significant attenuation of radon flux and gamma irradiation.
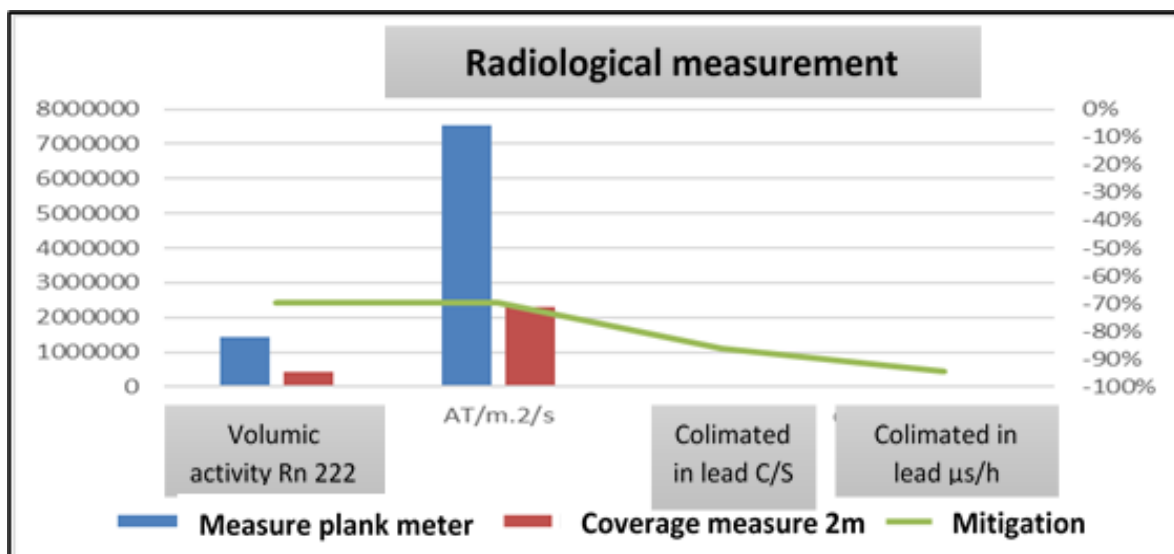

Figure 4. Representation of the radon activity volume and gamma radiation dispersion as a function of the thickness of the cover

3.5 Multivariate Statistical Analysis

3.5.1 Correlation analysis

The **Table 5** presents the results of the normality test used for the variables radon, temperature, humidity, gamma ray and altitude of measurements. The analysis of this table shows that all the significance values (Sig values) of the variables obtained using the Kolmogorov-Smirnova and Shapiro-Wilk methods are lower than 0.05. Thus, these Sig values indicate that the variables radon, temperature, humidity, gamma ray and altitude of the measurement points do not have a normal distribution. Therefore, Spearman's method, which is a non-parametric method is more suitable for correlation analysis of these variables [42].

Table 5. Normality test result

	Kolmogorov-Smirnova			Shapiro-Wilk		
	Statistic	*df*	*Sig.*	*Statistic*	*df*	*Sig.*
Radon (Bq/m3)	0,257	266	0	0,649	266	0
Temperature(°C)	0,123	266	0	0,949	266	0
Moisture (%)	0,112	266	0	0,938	266	0
γ (mS/h)	0,4	266	0	0,544	266	0
Altitude (m)	0,409	266	0	0,659	266	0

Table 6 shows the Spearman correlation matrix for the values of radon, temperature, humidity, gamma ray and altitudes of the measurement points measured in the study area during this work. The value of the correlation coefficient is a good indicator of the relationship between the variables. When this R value is close to 0, it means that there is no correlation or link between the variables concerned. An R value greater than 0.7 indicates a strong correlation between the variables and an R value between 0.5 and 0.7 indicates a medium correlation between the variables. A very high value (r = + 1 or - 1) of R indicates a perfect correlation between the variables concerned [43, 44, 45].

Table 6. Spearman correlation analysis results

Parameters	Radon (Bq/m3)	Temperature (°C)	Moisture (%)	γ (mS/h)	Altitude (m)
Radon (Bq/m3)	1	-0,757**	0,608**	0,381**	-0,381**
Temperature(°C)	-0,757**	1	-0,858**	- 0,088	0,088
Moisture (%)	0,608**	-0,858**	1	- 0,182**	0,182**
γ (mS/h)	0,381**	-0,088	-0,182**	1	-0,99**
Altitude (m)	-0,381**	0,088	0,182**	-0,99**	1
** Correlation is significant at the 0.01 level (2-tailed).					

The analysis of this table 6 shows that there is a very strong negative correlation between humidity and temperature (R = - 0.857), between temperature and radon concentrations (R = -0.757). The strong negative correlations observed between temperature and humidity on the one hand, and between temperature and radon concentrations on the other hand, clearly indicate that temperature has an influence on radon concentrations and humidity. Thus, an increase in temperature could lead to a decrease in radon concentrations and humidity and vice versa. A very low correlation was observed between temperature and gamma radiation (R = -0.088) and between humidity and gamma radiation (R = -0.182). These low correlation values observed indicate that the values of humidity and

temperature have no influence on the gamma radiation of the study area. A weak correlation was observed between gamma radiation and radon concentrations (R = - 0.381) and between altitude and radon (R = - 0.381). A very strong negative correlation was observed between altitude and gamma radiation (R = - 0.99). This high correlation value observed between the values of altitude and gamma radiation indicates that these two variables move almost perfectly together but in reverse order.

3.5.2 *Principal Component Analysis*

In this study, the principal component analysis method was used to determine the relationship between radon concentrations, gamma radiation values, altitude values, temperature values and humidity values. The results of the KMO and Bartlett tests applied to the variables are presented in **Table 7**. This table shows that the KMO value of the data used for the principal component analysis is 0.595. The significance value for Bartlett test is 0; therefore, the data are suitable for principal component analysis. The values of total variance explained, eigenvalues, cumulative % of variance and factor loading in rotation for each principal component were summarized in **Table 8**. The spatial distribution of the principal components is given in **Figure 5**. According to the results of the principal component analysis, two principal factors with eigenvalues greater than one (1) were formed. These two factors alone explain 85.31% of the total variance. The first factor alone accounts for 46.84% of the variance and the second factor accounts for 38.191% (**Table 8**). The results of this analysis revealed that factor 1 which accounts for 46.84% of the total variance is mainly related to a high positive loading of gamma radiation and a high negative loading of altitude values. This confirms the results of the correlation analysis obtained earlier where a very strong correlation coefficient was obtained between the gamma radiation and the altitude values. The factor 2 which represents 38.191% of the total variance is mainly related to a strong positive loading of humidity (0.929), temperature (- 0.926) and a medium positive loading of radon (0.601). These results also confirm the results of the correlation analysis obtained earlier where significant correlation coefficient values were obtained between these variables.

Table 7. KMO and Bartlett's Test

Kaiser-Meyer-Olkin Measure of Sampling Adequacy.		0,595
Bartlett's Test of Sphericity	Approx. Chi-Square	795,165
	df	10
	Sig.	0

Table 8. Rotated factor loading, total variance explained, and eigenvalues of each factor

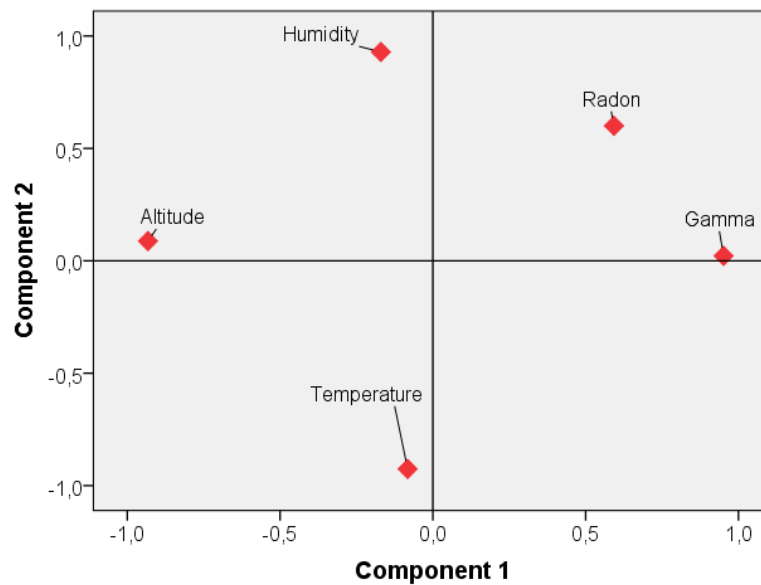| Parameters	Component	
	1	2
Gamma radiation	0,952	0,022
Altitude	-0,932	0,088
Humidity	-0,17	0,929
Temperature	-0,083	-0,926
Radon	0,593	0,601
Eigen values	2,342	1,91
% of Variance	46,84	38,191
Cumulative %.	46,84	85,031

Figure 5. Spatial distribution of principal components

Conclusion

This study focused on the assisted radiological stabilization of radon fluxes and gamma irradiations of tailings from the processing of uranium ore in the Arlit mines. The radon concentration values in the work environment vary between 0 and 7400 Bq/m3 with an average of 804.88 Bq/m^3). Those of gamma γ radiation vary from 1.26 to 4.16 mS/h. Humidity and temperature values measured during this period vary respectively from 6 to 39% for humidity; and from 26.6 to 49.5°C for temperature. The slope is rehabilitated by placing the slope on an impermeable clay surface with a permeability of k < 10^{-8} m/s ; by placing a geomembrane on the clay layer to ensure the watertightness of the barrier, then by determining the integrating slope of the slope of the slope not exceeding 30 degrees and allowing to have a safety coefficient f ≥ 1.5 to have a good stability of the slope and finally by dividing the main slope into several sub-slopes called redans with a slope < 15 degrees. The permeability values at temperature T of the Tejia Clay and Abinky Sandstone used for the reclamation and containment of the tailings piles from the ore processing in the study area vary between 0.005.10^{-7} and 0.0016.10^{-7} m/s with an average of 1.33.10^{-8} m/s. The permeability values at 20℃ permeability values are lower than those measured previously. The porosity values vary between 14.29 and 17.92. These low permeability and porosity values indicate that the samples are sufficiently suitable for containment of the study area slurries. The gamma radiation and radon measurements are very low after the 2m cover. The average attenuation is between 70% and 92%. Radon is down by 70% for a 94% decrease for gamma in μSv/h. The principal component analysis highlighted two main groups of factors. The first factor is mainly related to a strong positive loading of gamma radiation and a strong negative loading of altitude values. While the second Factor 2 is mainly related to a strong positive loading of humidity, temperature and a medium positive loading of radon.

Acknowledgement

References

[1] D. Dewar, L. Harvey, and C. Vakil "Uranium mining and health" Canadian Family Physician, 59(5) (2013) e215-e217.

[2] A. Diallo "Les Facteurs Historico-Geographiques De La Crise Securitaire Au Sahel : Case Du Burkina Faso, Mali et Niger " Crisis Communication and Conflict Resolution in Francophone Africa, 70.

[3] D. Brugge, J.L. deLemos, and B. Oldmixon "Exposure pathways and health effects associated with chemical and radiological toxicity of natural uranium : a review " Reviews on environmental health, 20(3) (2005) 177-194.

[4] E.S. Craft, A.W. Abu-Qare, M.M. Flaherty, M.C. Garofolo, H.L. Rincavage, and M.B. Abou-Donia "Depleted and natural uranium : chemistry and toxicological effects" Journal of Toxicology and Environmental Health, Part B, 7(4) (2004) 297-317.

[5] A.V. Nesterenko, V.B. Nesterenko, and A.V. Yablokov "Chapter II. Consequences of the Chernobyl catastrophe for public health" Annals of the New York Academy of Sciences, 1181(1) (2019) 31-220.

[6] A.V. Yablokov, V.B. Nesterenko, and A.V. Nesterenko "Chapter III. Consequences of the Chernobyl catastrophe for the environment" Annals of the New York Academy of Sciences, 1181(1) (2009) 221-286.

[7] F. Lahyani " Contribution Méthodologique Aux Études D'Impact Environnemental Et Social Des Projets De Mines D'uranium Au Québec" (2020).

[8] P.L Auger, I. Gingras, M.A. Duguay, B. Imbeault, J. Levasseur and, É. Notebear "Uranium Exploration and Mining : Why We Demand a Moratorium. Ministère du Développement durable, de l'Environnement, de la Faune et des Parcs" (2010) Retrieved from http://www.protegerlenord.mddep.gouv.qc.ca/memoires/medecins-sept-iles.pdf

[9] C. Murray "Environmental impacts and mitigation measures related to uranium exploration and mining" Doctoral dissertation, publisher not identified, (2014).

[10] C. Balegamire, B. Nkuba and P. Dable (2022) "Production of gold mine tailings based concrete pavers by substitution of natural river sand in Misisi, Eastern Congo" Cleaner Engineering and Technology, 7 2022 100427.

[11] R.J. Bissett, and J.R. McLaughlin "Radon"*Chronic Dis Can*, *29*(1) (2010) 38-50.

[12] SFDA "Biological Effects of Ionizing Radiation; United States Food and Drug Administration" HEW Publication (FDA): Silver Spring, MD, USA, 2006 77–8004.

[13] IAEA "*Radiation Protection and Safety of Radiation Sources: International Basic Safety Standards*; IAEA Safety Standards Series" International Atomic Energy Agency: Vienna, Austria, 2014.

[14] L.B. Zablotska, R.S. Lane and K. Randhawa "Association between exposures to radon and γ-ray radiation and histologic type of lung cancer in Eldorado uranium mining and milling workers from Canada" *Cancer*, *128*(17) 2022 3204-3216.

[15] E.K. Atibu, P. Arpagaus, C.K. Mulaji, P.T. Mpiana, J. Poté, J.L. Loizeau and F.P. Carvalho "High Environmental Radioactivity in Artisanal and Small-Scale Gold Mining in Eastern Democratic Republic of the Congo" *Minerals*, *12*(10) 2022 1278.

[16] E. Cléro, L. Marie, C. Challeton-De Vathaire, D. Laurier, and A. Rannou, "Assessment of radon-induced health risks for occupants of a house built on uranium ore tailings" *Journal of Epidemiology and Public Health*, 64(4) (2016) 237-246.

[17] H. Baysson, and M. Tirmarche "Lung cancer risk after radon exposure : state of epidemiological knowledge"*Archives des Maladies Professionnelles et de l'Environnement*, *69*(1) (2008) 58-66.

[18] S. Feng, D. Gao, F. Liao, F. Zhou, X. Wang "The health effects of ambient PM2. 5 and potential mechanisms" Ecotoxicology and environmental safety, 128 (2016) 67-74.

[19] O.K. Sidi-Tanko "Dynamics of vegetation in mining area in the urban commune of Arlit" Master's Thesis, Abdou Moumouni University of Niamey Niger (2012).

[20] AMAN" Etat des lieux de la qualité des nappes du Tarat et de l'Izegouande Synthèse des analyses chimiques et radiométriques disponibles à Décembre" (210) 1-98.

[21] SRK "Rapport d'Etude d'Impact Environnemental et Social sur le projet Madaouéla Ouest, Arlit, Niger final version" (2) (2015).

[22] F. Yaou Korgom " Hydrogeological and hydrogeochemical characterization of the groundwater in the Arlit Mining Zone in Niger" Final year work (2019).

[23] N. Ministry of Mines "Geological and Mining Research Master Plan (PDRGM) " 60 (2013) -202.

[24] M.S.H Rachid "Conceptualization of the water flow of the Tarat aquifer on the sector of SOMAIR" Thesis for the obtaining of the Master of Engineering (2013).

[25] J. Lang, M. Yahaya, M.O. El Hamet, J.C. Besombes, and M. Cazoulat "Lower Carboniferous Glacial Deposits in Western Aïr (Niger) " Geologische Rundschau, 80(3) (1991) 611-622.

[26] H. Darcy "*Les fontaines publiques de la ville de Dijon : Exposition et application des principes à suivre et des formules à employer dans les questions de distribution d'eau : Ouvrage terminé par un appendice relatif aux fournitures d'eau de plusieurs villes, au filtrage des eaux et à la fabrication des tuyaux de fonte, de plomb, de tôle et de bitume" V. Dalmont,* 2 (1856).

[27] A.A. Tadewal, B.D. Farida, K. Moussa and B. Ousmane "Hydrogeological characterization of the Izegouande Permian aquifer (Tim Mersoï Basin, North Niger) " American Journal of Sciences and Engineering Research, 4 (5) 2021 12-23.

[28] R.A. Freeze "Henry Darcy and the fountains of Dijon" *Groundwater*, *32*(1) (1994) 23-30.

[29] P. Stengel "Use of porosity system analysis for characterization of soil physical condition in situ" In *Annales agronomiques* 30 (1) (1979) 27-51.

[30] E. Recordon "Deformability of unsaturated soils at various temperatures" *Revue française de géotechnique*, (65) (1993) 37-56.

[31] R.B Roberts, R.C Meyer, and P. Wang "Further observations on the splitting of uranium and thorium" *Physical Review*, *55*(5) (1939) 510.

[32] O. K. Dessouky, and H.H Ali "Using Portable Gamma-Ray Spectrometry for Testing Uranium Migration : A Case Study from the Wadi El Kareim Alkaline Volcanics, Central Eastern Desert, Egypt" *Acta Geologica Sinica-English Edition*, *92*(6 (2018) 2214-2232.

[33] C. Ferry "*Radon-222 migration in soil. Application aux stockages de résidus issus du traitement des minerais d'uranium"* Doctoral dissertation, (2000) Paris 11.

[34] A. Kohn, and J. Ulmo "Some statistical considerations on the measurement of the activity of radioactive substances" *Journal of Applied Statistics*, *6*(2) (1958) 9-55.

[35] A. Axelsson, and A. Ringbom "On the calculation of activity concentrations and nuclide ratios from measurements of atmospheric radioactivity" *Applied Radiation and Isotopes*, 92 (2014) 12-17

[36] S. Darby, D. Hill, H. Deo, A. Auvinen, J.M. Barros-Dios, H. Baysson, and R. Doll "Residential radon and lung cancer-detailed results of a collaborative analysis of individual data on 7148 persons with lung cancer and 14 208 persons without lung cancer from 13 epidemiologic studies in Europe " *Scandinavian journal of work, environment & health*, (2006)1-84.

[37] A. Gray, S. Read, P. McGale, and S. Darby "Lung cancer deaths from indoor radon and the cost effectiveness and potential of policies to reduce them" *Bmj*, (2009)*338*.

[38] S. Darby "Residential radon, smoking and lung cancer" *Radiat Res*, 163(6) (2005) 696.

[39] D. Drubay, "*Dose-response analysis for cancer and circulatory disease mortality risks in uranium miners"* Doctoral dissertation, Université Paris Sud-Paris XI, 2015.

[40] F. Beck, J.B. Richard, A. Deutsch, T. Benmarhnia, P. Pirard, C. Roudier, and P. Peretti-Watel "Knowledge and perception of radon risk in France" *Cancer/Radiotherapy*, *17*(8) (2013) 744-749.

[41] D. Bard, M. Tirmarche, P. Pirard "Radon exposure and public health risks" In *Annales pharmaceutiques françaises,* 58 (6) (2000) 373-382.

[42] O. Catelinois, A. Rogel, D. Laurier, S. Billon, D. Hemon, P. Verger, and M. Tirmarche "Lung cancer attributable to indoor radon exposure in France : impact of the risk models and uncertainty analysis" *Environmental health perspectives*, 114(9) (2006) 1361-1366.

[43] A.M. Hassan, A. Ersoy, and N.A. Turan "Assessment of heavy metal (loid) s in groundwater by multivariate statistical analysis and metals pollution indices : a case study of Çarşamba coastal aquifer, North Turkey " *Arabian Journal of Geosciences*, 14(23) (2021) 1-21.

[44] V. Satish Kumar, B. Amarender, R. Dhakate, S. Sankaran, and K. Raj Kumar "Assessment of groundwater quality for drinking and irrigation use in shallow hard rock aquifer of Pudunagaram, Palakkad District Kerala" *Applied Water Science*, 6(2) (2016) 149-167.

[45] A.M Hassan, and A. Firat Ersoy "Statistical assessment of seasonal variation of groundwater quality in Çarşamba coastal plain, Samsun (Turkey) " *Environmental Monitoring and Assessment*, 194(2) (2022) 1-29.

(2022); http://www.jmaterenvironsci.com